

GALACTIC BLACK HOLE BINARY SYSTEMS

C. Done¹

¹*Department of Physics, University of Durham, South Road, Durham, DH1 3LE, UK*

ABSTRACT

I review observations of the X-ray spectra of Galactic Black Hole Candidates, and theoretical ideas as to how these can be produced. X-ray reflection should enable different source geometries to be distinguished, but the ionisation instability of X-ray irradiated material in hydrostatic equilibrium gives rise to large ambiguities in interpretation. It is not currently possible to determine whether the underlying emission mechanism in the low state is an advective flow or magnetic reconnection above the disk, but more detailed modelling of the ionisation instability *may* allow us to distinguish between these scenarios.

INTRODUCTION

Accretion onto a black hole is observed to produce copious X-ray emission. At high mass accretion rates (approaching the Eddington limit) the spectra are dominated by a soft component at $kT \sim 1$ keV which is strongly (very high state: VHS) or weakly (high state: HS) Comptonized by low temperature thermal (or quasi-thermal) electrons with $kT \sim 5 - 20$ keV (e.g. Gierliński et al., 1999). There is also a rather steep power law tail ($\Gamma \sim 2 - 3$) which extends out beyond 511 keV in the few objects with good high energy data (e.g. Grove et al., 1998). At lower mass accretion rates, below $\sim 2 - 3$ per cent of Eddington (Życki et al., 1998; Gierliński et al., 1999), there is a rather abrupt transition when the soft component drops in temperature and luminosity. Instead this (low state: LS) spectrum is dominated by thermal Comptonization, with $\Gamma < 1.9$, rolling over at energies of ~ 150 keV (see e.g. the reviews by Tanaka & Lewin 1995; van der Klis 1995; Nowak 1995). This spectral form seems to continue even down to very low luminosities (~ 0.01 per cent of Eddington: the quiescent or off state e.g. Kong et al. 2000). These very different spectra can all be seen from a single object where the mass accretion rate changes substantially. Figure 1 (left panel) shows VHS, HS and LS spectra from the GBHC transient RXTE J1550-564.

Intriguingly, other accreting systems show the same sort of hard-to-soft spectral switch. The low magnetic field neutron star systems (atolls) show such a transition at $\sim 0.8 - 1$ per cent of Eddington (Ford et al., 2000), i.e. a factor of 2-3 lower than the GBHC. In AGN, nearby Seyfert galaxies generally have hard X-ray spectra which are rather similar to the LS GBHC spectra (Zdziarski et al 1995), while the (probably higher mass accretion rate) Narrow Line Seyfert 1 galaxies and radio quiet quasars look more similar to the HS/VHS spectra (e.g. the review by Życki 2000, these proceedings).

HARD X-RAY EMISSION MECHANISMS

The standard accretion disk models (Shakura & Sunyaev 1973; SS) cannot produce hard X-ray emission. Some additional process is required where a large fraction of the gravitational energy released by accretion is dissipated in an optically thin environment. For the SS disk, an obvious candidate is that there are magnetic flares above the disk, generated by the Balbus-Hawley MHD dynamo responsible for the disk viscosity (e.g. the review by Balbus & Hawley 1998). Buoyancy could cause the magnetic field loops to rise up to the surface of the disk, so they can reconnect in regions of fairly low particle density. Numerical simulations (albeit incomplete) do show this happening, although they do not yet carry enough power to reproduce the observed low/hard state (Miller & Stone 2000).

Such mechanisms change the SS disk structure, as much of the power is dissipated in a magnetic corona rather than in a disk (which is then cooler and denser: Svensson & Zdziarski 1994). However, the strong illumination of the disk by the corona also changes its structure to some (as yet not well understood) extent.

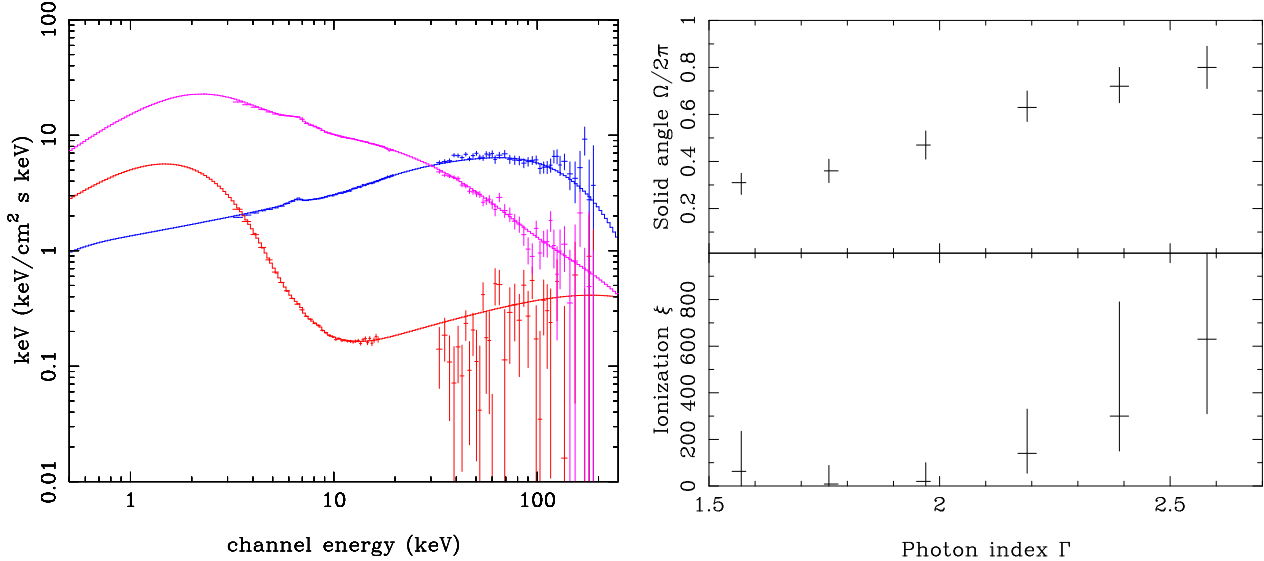


Fig. 1. Left panel: RXTE PCA and HEXTE data from RXTE J1550–564 showing the Low state (peaking at 100 keV), High state (sharply peaking at 1 keV) and very high state (smooth peak at 1 keV). Right panel: Fixed density reflection models fit to simulated spectra calculated from X–ray illuminated disk models including the self–consistent density structure (NKK). The ionisation instability forms an ionised skin on top of the disk which is completely reflective for flat spectrum illumination (high Compton temperature), so suppressing the observed reflected signature. For steeper spectra the skin depth decreases (from Done & Nayakshin 2000).

Little is known about the spectrum expected from electrons heated through magnetic reconnection, but the observed weak disk emission in the LS can be explained if most of the viscous dissipation is released in a patchy or outflowing magnetic corona (Svensson & Zdziarski 1994; Stern et al 1995; Beloborodov 1999). Thus it seems likely that such mechanisms could work to form the LS hard X–ray emission. However, there could be considerable problems in extending these ideas to the much lower luminosity quiescent X–ray state as numerical simulations of the MHD turbulence imply that the magnetic field shuts off when the disk material becomes mainly neutral as in quiescence (Gammie & Menou 1998; Fleming et al., 2000).

An alternative to the SS disk models is that the inner disk is replaced by an optically thin, X–ray hot accretion flow. By contrast with the magnetic reconnection models, these have spectra which can be worked out in some detail, typically giving electron temperatures of ~ 100 keV (advection dominated accretion flows: Narayan & Yi 1995). These can exist only at fairly low mass accretion rates as they rely crucially on the assumptions that the accretion energy is given mainly to the protons, and that the electrons are only heated via Coulomb collisions. At high densities (i.e. high mass accretion rates) the electrons efficiently drain energy from the protons and the flow collapses back into an SS disk at luminosities of $\sim \alpha_{0.1}^2$ per cent of Eddington (Esin et al., 1997; Quataert & Narayan 1999). These flows are also stable to convection (Narayan, Igumenshchev & Abramowicz 2000) at the high viscosity ($\alpha \sim 0.2$) required to get the LS–HS/VHS transition at the observed luminosities. Hence these flows could produce both the quiescent and LS spectra, and a physical mechanism for the HS/VHS state transition (Esin et al., 1997).

Magnetic reconnection is really the only known mechanism that can give the power law tail seen in the HS/VHS. There is also a radio jet/outflow seen in the VHS (and LS) but this is strongly quenched in HS (e.g. Fender 2000) while the hard X–ray tail can stay relatively constant (e.g. left panel of Figure 1). An alternative possibility is that the hard X–ray tail comes from the accelerating infall between the last stable orbit and the event horizon. Compton scattering from the bulk motion of the accelerating flow can upscatter any seed photons intercepted by this material into a power law tail. However, the free–fall electron velocities are not high enough (typical velocities of $\sim 0.7c$ imply Lorentz factors of only $\gamma \sim 1.4$) to extend the power law past $\sim 100 - 300$ keV (e.g. Laurent & Titarchuk 1999, Zdziarski 2000) yet the highest signal–to–noise HS/VHS spectra extend unbroken beyond this (e.g. Grove et al 1998).

There is also some thermal Comptonization of the disk photons in the HS and (most strongly) VHS

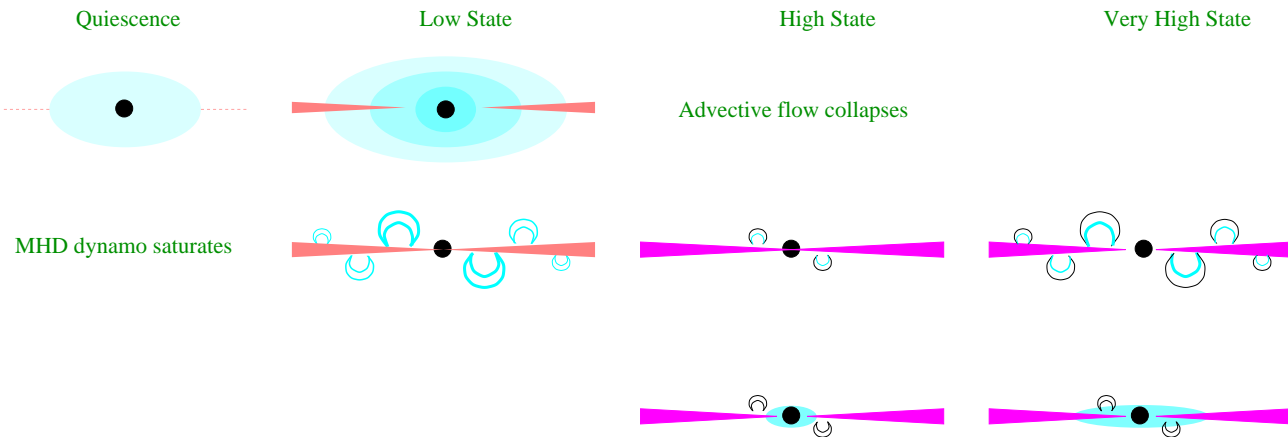


Fig. 2. Potential X-ray emission mechanisms in the various spectral states. In quiescence the disk is NOT in steady state (as indicated by the dotted line). Hydrogen is mostly neutral and the MHD dynamo probably cannot operate. In the low state the accretion flow is in (quasi)steady state. Hydrogen is ionised so the MHD dynamo works, and if there is reconnection above the disk then this could heat the electrons. Alternatively, the X-ray emission in both quiescence and low state could be powered by an advective flow. In the high and very high states the only serious contender for the hard power law tail is magnetic reconnection leading to a non-thermal electron distribution (indicated by the black loops), while the thermal electrons could be part of the same mechanism (grey loops) or could be associated with the inner disk.

(Gierliński et al., 1999, Wilson & Done 2000). This could be due to heated upper layers of the inner disk, Comptonizing the radiation from beneath as it escapes (e.g. Życki et al., 1999b). Alternatively, magnetic reconnection above the disk could produce both the non-thermal and thermal electron distributions (hybrid plasma: Poutanen & Coppi 1998; Gierliński et al., 1999).

Figure 2 sketches all these potential hard X-ray emission mechanisms for each state.

TESTING THE MODELS

These very different mechanisms for the hard X-ray emission also imply very different geometries (see Figure 2). If there was a way to constrain the hard X-ray source geometry then we could start to distinguish between the emission mechanisms. The overall continuum shape gives the first constraints as the Comptonised spectrum is determined by the ratio of power in the seed photons to that in the hard electrons (e.g. Haardt & Maraschi 1993; Poutanen et al 1997).

Variability Behaviour

Another potential diagnostic is from the variability behaviour of the source, since their power spectra show characteristic frequencies in the form both of breaks and Quasi Periodic Oscillations (QPO's). These features are related ($f_{break} \sim 10f_{QPO}$ for the low frequency QPO), and they *move*, with the frequencies generally being higher (indicating smaller size scales) as the source changes from LS to VHS (see e.g. the review by van der Klis 2000). However, the physical origin of these features are not well understood, and there are several models for QPO formation (see e.g. the review by van der Klis 2000). Recent progress has concentrated on the similarity between the relationship between the QPO and break frequencies in black holes *and* neutron star systems (Psaltis, Belloni & van der Klis 1999). If they truly are the same phenomena then the mechanism *must* be connected to the accretion disk properties and not to the magnetosphere or surface of the neutron star. One very promising approach is identifying the (low frequency) QPO's with the vertical precession timescale of a tilted ring of gas at the inner radius of the disk (Stella & Vietri 1998). This model was extended by Psaltis & Norman (2000), who calculated the transfer function of the disk to a spectrum of perturbations, showing that the disk acts as a low pass filter, with the hydrodynamic timescale at the inner edge suppressing fast variability (and so producing a low frequency break), with a superimposed QPO at the Lense-Thirring precession timescale. While this is tantalisingly close to observations, there are still some significant problems – most importantly connected to the neutron star spin frequencies which may have been measured during X-ray bursts (e.g. van der Klis 2000). However, despite these uncertainties, *all*

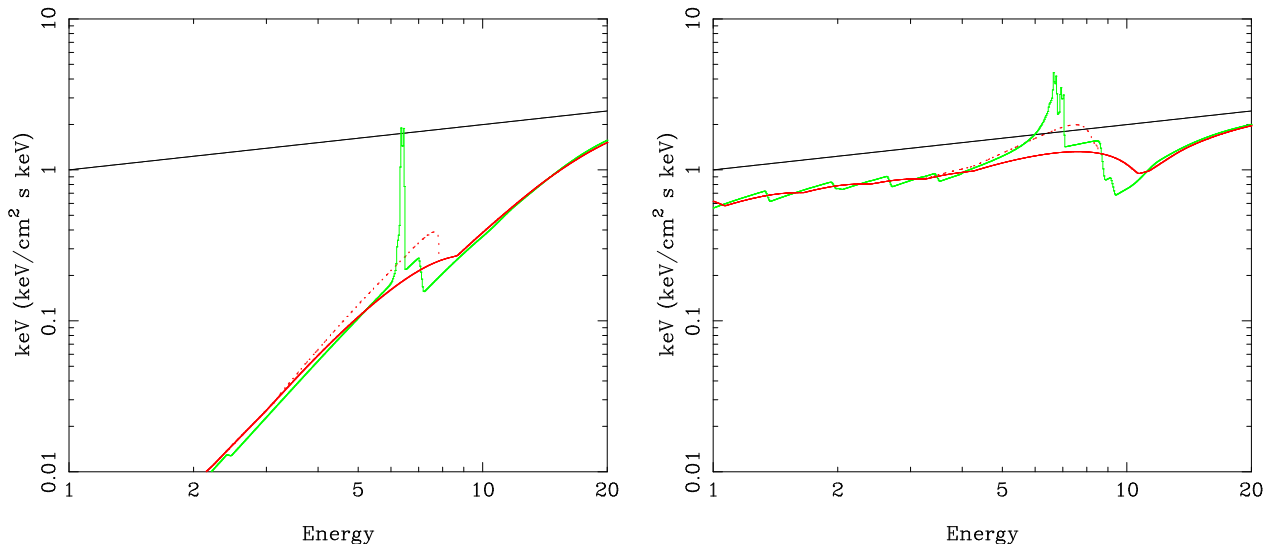


Fig. 3. Left panel: The light grey (green) line shows the $\nu f(\nu)$ spectrum reflected from a slab of neutral material of solar abundance viewed at 60° . The dark grey (red) line shows the same spectrum but from a disk extending down to the last stable orbit around a black hole (solid line is continuum only, while dotted line is continuum plus line). The black line is the illuminating spectrum. Right panel: As in (a) but for highly ionised material

QPO and break frequency models use a sharp transition in the accretion disk in some form to pick out a preferred timescale, so this should give *some* constraints on the geometry.

Reflected Spectra

Yet another, independent test of the geometry comes from the X-ray spectroscopy. Wherever hard X-rays illuminate optically thick material then a reflected spectrum is produced which has a characteristic spectral shape, with an especially prominent iron $K\alpha$ iron fluorescence line. The amount of line and reflected continuum depend on the solid angle subtended by the material, the ionization state and elemental abundances of the reflector (Lightman & White 1988; George & Fabian 1991; Matt, Perola & Piro 1991; Ross & Fabian 1993; Życki & Czerny 1994).

The reflected spectrum (line and continuum) is smeared by special and general relativistic effects of the motion of the disk in the deep gravitational potential well (Fabian et al., 1989). The fraction of the incident flux which is reflected gives a measure of the solid angle of the optically thick disk as observed from the hard X-ray source, while the amount of smearing shows how far the material extends into the gravitational potential of the black hole.

The left panel of Figure 3 shows the reflected spectrum from a slab of neutral, solar abundance material viewed at 60° (light grey/green) compared to that from a disk extending down to 3 Schwarzschild radii around a black hole. The Greens functions for the reflected continuum are taken from Magdziarz & Zdziarski (1995), which include Compton downscattering at all energies. The iron line is calculated self consistently with the continuum reflection (including Compton downscattering on the line profile) using the code of Życki & Czerny (1994), and the whole spectrum (line and continuum) is smeared assuming that the flux irradiating the accretion disk $F_{irr} \propto r^{-3}$ (see Appendix A of Życki et al., 1999).

The right panel of Figure 3 shows the same for a highly ionised reflector. The resulting spectrum now depends strongly on details of the assumed ionization structure, both as a function of height and of radius. Here we assume that the slab has a constant ionization parameter $\xi = L/(nr^2)$ (where L is the illuminating luminosity, at a distance r from the reflector of constant density n). The photo-electric opacity is calculated by determining the ion populations (balancing photo-ionization with collisional recombination as in Done et al., 1992). The electron temperature may then cause appreciable Compton upscattering (Ross & Fabian 1993; Ross, Fabian & Young 1999). This is *not* included in the reflected continuum calculation (Magdziarz & Zdziarski 1995), although it is included to some extent in the line profile (Życki & Czerny 1994 but see the discussion in Ross et al., 1999).

As can be seen from these figures, the fraction of reflected flux in the 1–20 keV band is dependent on the ionization state of the material as well as the solid angle subtended by it. The ionization state is determined mostly by the line and edge energies (although the reflection continuum shape is also important). But these energies can be shifted by relativistic effects (Ross, Fabian & Brandt 1996). Thus all three parameters (solid angle, ionization state and relativistic smearing) should be fit simultaneously in order to determine the geometry of the system.

COMPARISON WITH OBSERVATIONS OF GBHC: QUIESCENCE AND LOW STATE

The quiescent spectra are too faint to do detailed spectral fitting or variability power spectra, but they do appear to be hard $\Gamma < 2$ i.e. to be related to the LS spectra (e.g. Kong et al., 2000). There is much more information on the (much brighter) LS spectra.

Continuous static magnetic corona

The LS spectra are relatively hard $\sim 1.5 < \Gamma < 1.9$ extending out to $\sim 100 - 200$ keV, which is an immediate problem for a ‘disk–corona’ geometry where the magnetic flares are close enough together to form a quasi–continuous corona above the disk. In such a geometry, the hard X–ray corona radiates about as much power down towards the disk as up towards the observer. The downwards flux illuminates the disk, and some fraction (given by the energy integrated reflection albedo) is reflected but the rest is thermalised in the disk, forming an additional seed photon source (Haardt & Maraschi 1993). The reflection albedo cannot approach unity even if the disk is completely ionised due to Compton downscattering of the high energy spectrum. For $\Gamma = 1.5$ the maximum albedo ~ 0.5 , so the *minimum* soft seed flux is approximately a quarter of the hard luminosity. Yet this ratio of soft–to–hard flux would result in a Compton spectrum with $\Gamma \sim 1.8 - 1.9$ (Haardt & Maraschi 1993; Poutanen 1998). Thus the ‘disk–corona’ geometry is ruled out. If the magnetic corona exists, it must be patchy (Stern et al 1995; Gierliński et al., 1997).

Patchy static magnetic corona

The solid angle subtended by a disk below a (static) patchy corona would be $\sim 2\pi$. Clearly this can be tested by looking at the amount of reflection, which is easily seen in the LS spectra (e.g. Done et al., 1992). Fitting simultaneously for the solid angle, ionization state and relativistic smearing gives that the reflector subtends a solid angle of $< 2\pi$, is predominantly neutral, and significantly broadened but *not* by as much as expected if the reflecting material extended down to the last stable orbit (Życki et al., 1997; 1998; 1999; Done & Życki 1999). This means that fitting without including the effects of relativistic smearing and/or ionization does not lead to large distortions of the derived parameters. Fitting only for solid angle and ionization (Gierliński et al., 1997; Zdziarski, Lubiński & Smith 1999) or for solid angle and smearing (approximated by a Gaussian: Gilfanov et al., 1999; Revnivtsev et al., 2000), show overwhelmingly that the solid angle is significantly less than 2π , correlated with the spectral index in the sense that harder continua show smaller reflected fractions (Zdziarski et al., 1999; Gilfanov et al 1999; Revnivtsev et al 2000), *and* a smaller amount of smearing of the spectral features (Gilfanov et al 1999; Revnivtsev et al 2000).

These correlations extend to the time domain. Frequency resolved spectra show that the fastest variability is characterised by a flatter spectrum and lower reflected fraction (Revnivtsev et al., 1999). Also, the characteristic break frequency in the LS variability power spectra *increases* as the spectrum steepens and the reflected amplitude and smearing increase (Gilfanov et al 1999; Revnivtsev et al 2000).

The static patchy corona model above a mainly neutral disk is ruled out by the observations of $\Omega/2\pi < 1$ for hard spectra (see Beloborodov 2001, these proceedings). For magnetic coronae models to work then either the coronae are not static or the disk is ionized.

Outflowing magnetic corona

Outflow from magnetic reconnection is seen in the Sun, so it could also happen above the disk. If the outflow velocity is transrelativistic then the hard X–ray radiation from the reconnection is beamed away from the disk. This reduces the disk illumination, and thus the reflected fraction and the reprocessed soft seed photons. Faster outflow velocities then give fewer reprocessed soft photons and smaller reflected fractions (giving the $\Gamma - \Omega/2\pi$ correlation), and if these faster velocities are concentrated towards smaller radii then this would also suppress the relativistic smearing signature from the inner disk (Beloborodov 1999).

However, the mechanism for the spectral transition (LS–HS) is not entirely clear. Given that it seems likely that the HS/VHS emission is powered by reconnection, then it requires that the spectral transition is associated with the magnetic loops mainly reconnecting inside the optically thick material, rather than buoyantly rising above the disk. One potential trigger for this could be that the disk becomes radiation pressure dominated – although AGN disks are in general radiation pressure dominated yet can show hard spectra and low reflected fractions e.g. Zdziarski et al., (1999); Chiang et al., (2000); Done et al., (2000). Similarly the link to the variability power spectra is also not obvious: the particular radius picked out by the QPO/low frequency break cannot be the radius at which the disk becomes radiation pressure dominated as this would *increase* as the luminosity increases from LS–VHS while the power spectral features imply a *decreasing* radius.

Patchy corona above an ionised disk: I

This seems immediately ruled out by the observation that the reflected spectrum is mostly neutral in the LS. However, one way to suppress both line and reflected continuum is from a radial dependance of ionization state. If the inner region of the disk were so highly ionised that even iron is completely stripped then it produces no atomic features. Its reflected continuum is unobservable in the 2–20 keV range and it appears instead to be part of the power law continuum. The observed reflected spectrum could then come from material further out in the disk which is mostly neutral, and not highly relativistically smeared. Since the reflected fraction is the ratio of the observed reflection relative to the inferred incidence flux then $\Omega/2\pi$ is low both due to the inner disk solid angle being missed and because this unidentified reflected signature boosts the incident flux (Ross et al., 1999)

However, for a smooth (power law) distribution in ionization parameter with radius then between the extreme ionization inner disk and more neutral outer disk there must be an intermediate region of high ionization, where iron is mainly in H– and He–like ions. These produce huge spectral features (see figure 3, right panel), which are unmistakable. The ionised disk models can be split into radial zones of different ionization to test these ideas and in Cyg X–1 they can be shown to be incompatible with the data (Done & Życki 1999). Admittedly these models do not properly model the Compton upscattering of the edge features (and slightly underestimate the Compton broadening of the line: Ross et al., 1999) associated with the high ionization material, but this is probably not a large distortion.

Similarly, the assumption of a constant ionization parameter slab can (and should) break down in the vertical direction. Illumination of the surface of the disk can result in an extreme ionization skin, which is completely reflective. Some of the incident flux is reflected in the skin, reducing the irradiating flux in the lower layers, so their ionization state is smaller. Deep enough in the disk then the material can be mostly neutral, giving the observed reflected signature which has $\Omega/2\pi < 1$ as the illuminating flux for that layer is not the full incident flux and the apparent incident flux is boosted by the featureless reflected flux from the extremely ionised upper skin (Ross & Fabian 1993; Ross et al., 1999). Again though, there are problems with the intermediate ionization layers. If the ionization parameter varies smoothly as a (power law) function of height in the disk then between the extreme ionization and mostly neutral material there should be the highly ionised H– and He– like iron, with its unmistakable reflected spectral features. However, Comptonization is now much more of a problem as this spectrum has to be transmitted upwards through the extremely ionised, hot skin. This additional Compton broadening *may* be able to smear these features enough to disguise their presence. Such models have yet to be tested against the data but it seems likely that if the Comptonization is strong enough to distort the H– and He– reflected spectrum then it should also distort the observed *neutral* reflection signature. This also has to be transmitted through (even more of) the Comptonizing layers, and yet it is easily detected.

Again in these models, as with the outflowing corona, there is no obvious trigger for the LS–HS transition or particular radius to use for the power spectral variability.

Patchy corona above an ionised disk: II

A far more wide-ranging problem with the ionised reflection models considered to date is that they *assume* a given density structure as a function of height. At best, the codes take this structure and then work out the temperature and ionization state of the material as a function of height. But X–ray illumination *changes* the density structure of the material. Material at the top of the disk is heated by the illumination, and so

can expand, lowering its density. Deeper into the disk there is less X-ray heating, so the material is cooler, and hence denser.

The self-consistent density structure is especially important as there is a thermal ionization instability which affects X-ray illuminated material in pressure balance (Field 1965; Krolik, McKee & Tarter 1981; Kallman & White 1989; Ko & Kallman 1994; Rôżańska & Czerny 1996; Nayakshin, Kazanas & Kallman 2000, hereafter NKK). The disk is in hydrostatic equilibrium in the vertical direction, so the gas pressure, P_{gas} must increase with depth into the disk. In these circumstances, it is clearer to talk about the ionization structure in terms of the pressure ionization parameter $\Xi = P_{rad}/P_{gas}$ where $P_{rad} = L/(4\pi r^2 c)$ is the radiation pressure of the illuminating radiation (this relates to the density photo-ionization parameter $\xi \sim \Xi kT/(4\pi)$).

The X-ray heating clearly depends on height, with the material at the top of the layer being heated the most. Because the material is in pressure balance, the gas pressure is smallest at the top of the disk, so Ξ is at its maximum here. This corresponds to the uppermost stable branch of the ionization equilibrium S-curve on an $\Xi - T$ plot, with low density material which is highly or completely ionized. Atomic cooling is negligible so the temperature is a fraction of the local Compton temperature (see Krolik et al., 1981 and Nayakshin 2000); Compton heating is balanced by Compton cooling and bremsstrahlung. Going deeper down into the disk, the X-ray heating decreases with optical depth to electron scattering, τ_T , and the gas pressure increases. Hence, both the temperature and ionization parameter Ξ decrease. However, there is then a turning point on the S-curve, where the temperature and density are such that the rapidly increasing bremsstrahlung cooling causes the temperature to dramatically decrease. This pulls the gas pressure down, but hydrostatic equilibrium requires that the gas pressure must monotonically increase as a function of depth into the disk. The only way for the pressure to increase in a region with rapidly decreasing temperature is to rapidly increase the density, but this pushes up the cooling still further, and so decreases the temperature. Ionic and atomic species can now exist, so line transitions give a yet further increase in the cooling. Eventually this stabilises onto the bottom part of the S curve, where the X-ray heating is balanced primarily by line cooling from low temperature, high density material. This results in an almost *discontinuous* transition from a highly ionized, hot and relatively tenuous skin to mainly neutral, cool and relatively dense material.

Reflection can then be suppressed as in the previous section, by the decrease in illuminating flux on the neutral layer because of scattering in the ionised skin, and because the scattered (reflected) spectrum from the ionised skin is interpreted as incident continuum. The difference is that the ionization parameter can now make an *abrupt* rather than smooth transition from highly or extremely ionised to mostly neutral material (NKK).

The resulting reflected spectrum is crucially determined by the optical depth where this instability occurs *and* the Compton temperature of the skin (which depends on the illuminating power law as well as the local thermal disk spectrum). For hard spectra, $\Gamma \sim 1.6$, then the Compton temperature of the upper layer of the disk is high ~ 10 keV, its ionization is extreme so it produces no reflected spectral features. If the instability occurs after an optical depth of $\tau \sim 1$ then the apparent reflected fraction is ~ 0.2 from neutral material, as observed. For steeper spectra the Compton temperature of the upper layers drops. Thus the instability point occurs rather higher in the disk, so the optical depth of the skin decreases, and the amount of reflected flux increases (giving the $\Gamma - \Omega/2\pi$ correlation! NKK).

The right panel of Figure 1 shows results from fitting simulated 2–20 keV GINGA resolution spectra of these full vertical structure models with the fixed density reflection models. The apparent $\Gamma - \Omega/2\pi$ is clearly seen for the LS $\Gamma < 2$ spectra (Done & Nayakshin 2000).

These models concentrate on the vertical ionisation structure, but there should also be a radial dependence. Larger radii should be less ionised and the total disk spectrum is found by integrating over all these different ionisations. However, the meaning of less ionized is very different from that in the constant density models – the skin remains completely ionized with a negligible amount of H and He-like iron, but its Thomson depth decreases with radius (see Nayakshin 2000). Thus the inner disk can have a larger skin depth, so suppressing the most extreme relativistically smeared line components (Nayakshin 2000). Perhaps this also gives a radius where the skin depth changes from $\tau_T > 1$ to $\tau_T \ll 1$ which could pick out a characteristic frequency for the power spectral variability, although the mechanism for the LS–HS transition is again not clear (see previous section).

Truncated disk with inner X-ray hot flow

All the observations can all be qualitatively explained in the truncated disk–advective inner flow model, with the disk progressively penetrating further into the advective flow. The geometry automatically gives a rather ‘photon starved’ hard continuum. As the overlap between the two phases increases, the soft seed photon flux intercepted by the hot inner flow gets larger, and so leads to a steeper continuum. But the increasing overlap also gives a larger solid angle subtended by the disk (resulting in a $\Gamma - \Omega/2\pi$ correlation: Poutanen, Krolik & Ryde 1997). The decreasing inner radius of the disk also gives the increasingly relativistically smeared spectral features, *and* higher frequency power spectral features. The advective flow collapses at luminosities at a few per cent of Eddington, giving a physical mechanism for the state transition which is observed at these fluxes.

The only problem is a quantitative one. The inner disk radii deduced from the relativistic smearing are $\sim 10 - 20$ Schwarzschild radii. Standard advective flow calculations assume that the transition radius between the SS disk and hot inner flow is large $\sim 10^4$ Schwarzschild radii. This is an assumption, and can be changed. The transition radius can be physically determined by calculating the evaporation rate from the ionised disk skin (Różańska & Czerny 2000), but irrespective of the mechanism, moving the disk inwards (and especially increasing the overlap between the two flows) increases the soft seed photon flux intercepted by the advective flow, leading to stronger Compton cooling. Bringing the disk in to $\sim 10 - 20$ Schwarzschild radii lowers the maximum luminosity at which the advective flow can exist by a factor of 2–3 (Esin 1997), which then makes the LS–HS/VHS state transition at slightly lower luminosities than observed.

However, the ideas developed above about the ionization structure of the disk should also apply here. Any hydrostatic disk illuminated by hard X-rays is subject to the thermal instability, and so should have an ionised skin. The observed neutral reflected spectrum is transmitted through this skin, and is subject to Compton broadening. If some fraction of the width of the line is due to Compton scattering rather than relativistic effects then this would result in an underestimate of the disk radius, and so extend the maximum luminosity of the advective flow back into the observed range.

COMPARISON WITH OBSERVATIONS OF GBHC: HIGH AND VERY HIGH STATE

Much less work has been done on X-ray reflection in the soft states. The only spectra which have been analysed with both ionisation and relativistic smearing included in the reflected spectrum are Nova Muscae (Życki et al., 1998), RXTE J1550-564 (Wilson & Done 2000) and Cyg X-1 (Gilfanov et al., 1999; Gierliński et al 1999). Fitting with the fixed density/ionization structure models gives a solid angle of $\sim 0.2 - 1$ of strongly ionised material, and that the spectral features are strongly smeared. Fits which do not include ionisation of the reflector will *overestimate* the solid angle subtended by the reflecting material (compare the left and right panels of Figure 3), so the results of Gilfanov et al., (1999) on the $\Gamma - \Omega/2\pi$ – smearing correlations will probably change significantly for the steep spectrum objects in their sample when ionisation is included.

The true solid angle is again hard to infer due to ionization effects. Even with the fixed density reflection models it depends on how the ionization varies as a function of radius (Życki et al., 1998). Obviously the ionization can also vary as a function of height, and the ionization instability again should operate. For steep spectral illumination this does not generally lead to suppression of the observed reflected flux as the Compton temperature of the skin is not high enough to completely strip iron. Instead it is dominated by H- and He-like iron and so its reflected spectrum can be seen directly (Figure 1, right panel; Done & Nayakshin 2000). But yet another problem for the reflection models is that the disk should now be substantially collisionally ionised, as well as photo-ionised.

Even more uncertainty comes from the geometry. If the thermal/non-thermal electrons are co-spatial then both should illuminate the disk. But if only the non-thermal electrons are associated with magnetic reconnection, while the thermal electrons are from a heated disk skin then most of the incident flux for reflection will be only from the non-thermal power law, while the observed incident continuum below 20 keV can be dominated by the thermal Compton component. This would dilute the observed solid angle (Wilson & Done 2000; Gierliński et al., 1999), but the Compton continuum produced from a non-thermal electron distribution can be highly anisotropic, which could boost the observed solid angle (Ghisellini et al., 1991)!

CONCLUSIONS

GBHC show different spectral states which roughly correspond to luminosity, with the LS–HS/VHS transition occurring at 2–4 per cent of Eddington. In the LS ($1.5 < \Gamma < 1.9$), fitting the spectra with (fixed density) models of X–ray reflection gives that the solid angle subtended by the disk is small $\Omega/2\pi < 1$, that the material is mainly neutral, and that the spectral features are broadened, but not by as much as expected from relativistic effects if the disk extended down to the last stable orbit around the black hole. If the smearing is due to relativistic effects alone then it implies that the reflecting material only extends down to 10 – 20 Schwarzschild radii. All these correlate, with steeper spectra having more reflection and more broadening (and higher frequency features in the power spectra).

These observations rule out the continuous corona model (from the overall hard spectral shape) and a static patchy corona above a neutral disk (from $\Omega/2\pi < 1$) and a static patchy corona above an ionised disk (as the reflector is mainly neutral) and advective flows (from the combination of small inner radius and high luminosity). Only the outflowing corona (Beloborodov 1999) can fit these ‘observed’ parameters. Radial ionization structure is unlikely to change these conclusions, although vertical ionization structure can give some loopholes due to Compton scattering of the observed reflected signature (Ross et al., 1999). This *may* distort the reflected signature from a static patchy corona by enough to not see the high ionization zone, and Compton broadening *may* allow the advective flow inner radius to be significantly larger.

However, the constant density models can be seriously misleading due to the ionization instability (NKK). This can cause a discontinuous transition between an extremely ionised skin overlying mostly neutral material, and can reproduce the observations (and correlations) with a static patchy magnetic corona. But this instability should be present whatever the mechanism for illumination of the disk, so it can also co–exist with either an advective flow or an outflowing corona. This of course completely removes any diagnostic power from the fixed density reflection models (Done & Nayakshin 2000).

For the HS and VHS the reflected spectrum is plainly highly ionised and broadened. However, the solid angle is even less constrained than in the LS due to the complex continuum, which could represent a single thermal/non–thermal electron population or could represent two entirely spatially distinct regions, with different solid angles for illumination of the disk material.

Reflection *may* be able to live up to its promise of illuminating the geometry (and so distinguishing between various ideas as to the underlying emission mechanisms) but *only* with much more detailed modelling of the X–ray irradiated disk.

ACKNOWLEDGEMENTS

Much of this review includes ideas developed in collaborations with S. Nayakshin, C. Wilson and P. Życki.

REFERENCES

- Balbus S.A., and J.F. Hawley, Turbulent Transport in Accretion Disks, Accretion Processes in Astrophysical Systems, Eds: S.S. Holt & T.R. Kallman, *AIP Conference Proceedings*, **431**, 79–88, 1998.
- Beloborodov A.M., Plasma Ejection from Magnetic Flares and the X-Ray Spectrum of Cygnus X-1, *ApJ*, **510**, L123–L126, 1999.
- Chiang J., et al., Simultaneous EUVE/ASCA/RXTE Observations of NGC 5548, *ApJ*, **528**, 292–305, 2000.
- Done C., J.S. Mulchaey, R.F. Mushotzky, and K.A. Arnaud, An ionized accretion disk in Cygnus X-1, *ApJ*, **395**, 275–288, 1992.
- Done C., and P.T. Życki, Relativistic Distortions in the X–ray Spectrum of Cyg X-1, *MNRAS*, **305**, 457–468, 1999.
- Done C., G. Madejski, and P.T. Życki, The Relativistic Iron Line Profile in the Seyfert 1 Galaxy IC 4329A, *ApJ*, **536**, 213–224, 2000.
- Done C., and S. Nayaskin, , *ApJ*, in press, 2000.
- Esin A.A., J.E. McClintock, and R. Narayan, Advection-dominated Accretion and the Spectral States of Black Hole X-Ray Binaries: Application to Nova Muscae 1991, *ApJ*, **489**, 865–889, 1997.
- Esin A.A., Heating and Cooling of Hot Accretion Flows by Nonlocal Radiation, *ApJ*, **482**, 400–413, 1997.
- Fabian A.C., M.J. Rees, L. Stella, and N.E. White, X-ray fluorescence from the inner disc in Cygnus X-1, *MNRAS*, **238**, 729–736, 1989.
- Fender R.P., Energetics of jets from X-ray binaries, In Third Microquasar Workshop, Eds A. J. Castro-

- Tirado, J. Greiner and J. M. Paredes, *Astrophysics and Space Science*, in press, 2000.
- Field G.B., Thermal Instability, *ApJ*, **142**, 531-567, 1965.
- Fleming T.P., J.M. Stone, and J.F. Hawley, The Effect of Resistivity on the Nonlinear Stage of the Magnetorotational Instability, *ApJ*, **530**, 464-477, 2000.
- Ford E.C. et al., Simultaneous Measurements of X-Ray Luminosity and Kilohertz Quasi-Periodic Oscillations in Low-Mass X-Ray Binaries, *ApJ*, **537**, 368-373, 2000.
- Gammie C.F., and K. Menou, On the Origin of Episodic Accretion in Dwarf Novae, *ApJL*, **492**, L75-L78, 1998.
- George I.M., and A.C. Fabian, X-ray reflection from cold matter in active galactic nuclei and X-ray binaries, *MNRAS*, **249**, 352-367, 1991.
- Gierliński M., et al., Simultaneous X-ray and gamma-ray observations of CYG X-1 in the hard state by GINGA and OSSE, *MNRAS*, **288**, 958-964, 1997.
- Gierliński M., et al., Radiation mechanisms and geometry of Cygnus X-1 in the soft state, *MNRAS*, **309**, 496-512, 1999.
- Ghisellini G., I.M. George, A.C. Fabian, and C. Done, Anisotropic inverse Compton emission, *MNRAS*, **248**, 14-19, 1991.
- Gilfanov M., E. Churazov, and M. Revnivtsev, Reflection and noise in Cygnus X-1, *A&A*, **352**, 182-188, 1999.
- Grove J.E. et al, Gamma-Ray Spectral States of Galactic Black Hole Candidates, *ApJ*, **500**, 899-908, 1998.
- Haardt F. and L. Maraschi, X-ray spectra from two-phase accretion disks, *ApJ*, **413**, 507-517, 1993.
- Kallman T.R., and N.E. White, Iron K lines from low-mass X-ray binaries, *ApJ*, **341**, 955-960, 1989.
- King A.R., and H. Ritter, The light curves of soft X-ray transients, *MNRAS*, **293**, L42-L48, 1998.
- Ko Y.-K., and T.R. Kallman, Emission lines from X-ray-heated accretion disks in low-mass X-ray binaries, *ApJ*, **431**, 273-301, 1994.
- Kong A.K.H., E. Kuulkers, P.A. Charles P.A., and L. Homer, The 'off' state of GX339-4 2000, *MNRAS*, **312**, L49-L55, 2000.
- Krolik J.H., C.F. McKee, and C.B. Tarter, Two-phase models of quasar emission line regions, *ApJ*, **249**, 422-442, 1981.
- Laurent P., and L.G. Titarchuk, The Converging Inflow Spectrum Is an Intrinsic Signature for a Black Hole: Monte Carlo Simulations of Comptonization on Free-falling Electrons, *ApJ*, **511**, 289-297, 1999.
- Lightman A.P., and T.R. White, Effects of cold matter in active galactic nuclei - A broad hump in the X-ray spectra, *ApJ*, **335**, 57-66, 1988.
- Magdziarz P., and A.A. Zdziarski, Angle-dependent Compton reflection of X-rays and gamma-rays, *MNRAS*, **273**, 837-848, 1995.
- Matt G., G.C. Perola, and L. Piro, The iron line and high energy bump as X-ray signatures of cold matter in Seyfert 1 galaxies, *A&A*, **247**, 25-34, 1991.
- Miller K.A. and J.M. Stone, The Formation and Structure of a Strongly Magnetized Corona above a Weakly Magnetized Accretion Disk, *ApJ*, **534**, 398-419, 2000.
- Narayan R., and I. Yi, Advection-dominated Accretion: Underfed Black Holes and Neutron Stars, *ApJ*, **452**, 710-735, 1995.
- Narayan R., Igumenshchev I.V., Abramowicz M.A., Self-similar Accretion Flows with Convection, *ApJ*, **539**, 798-808, 2000.
- Nayakshin S., D. Kazanas, and T.R. Kallman, Thermal Instability and Photoionized X-Ray Reflection in Accretion Disks, *ApJ*, **537**, 833-852, 2000.
- Nayakshin, S. On the X-Ray-heated Skin of Accretion Disks, *ApJ*, **534**, 718-722, 2000.
- Nowak M.A., Toward a Unified View of Black-Hole High-Energy States, *PASP*, **107**, 1207-1214, 1995.
- Poutanen J., Accretion disk corona models and the X-gamma-ray spectra of accreting black holes, In Theory of Black Hole Accretion Discs, CUP, Cambridge, p100-122, 1998.
- Poutanen J., and P.S. Coppi, Unification of Spectral States of Accreting Black Holes, *Physica Scripta*, **T77**, 57-59, 1998.
- Poutanen J., J.H. Krolik, and F. Ryde, The nature of spectral transitions in accreting black holes - The case of CYG X-1, *MNRAS*, **292**, L21-L25, 1997.

- Psaltis D., T. Belloni, and M. Van der Klis, Correlations in Quasi-periodic Oscillation and Noise Frequencies among Neutron Star and Black Hole X-Ray Binaries, *ApJ*, **520**, 262-270, 1999.
- Psaltis D., and Norman C., On the Origin of Quasi-Periodic Oscillations and Broad-band Noise in Accreting Neutron Stars and Black Holes, *ApJ*, submitted, 2000.
- Quataert E., and R. Narayan, On the Energetics of Advection-dominated Accretion Flows, *ApJ*, **516**, 399-410, 1999.
- Revnivtsev M., M. Gilfanov, and E. Churazov, The frequency resolved spectroscopy of CYG X-1: fast variability of the Fe K α line, *A&A*, **347**, L23-L26, 1999.
- Revnivtsev M., M. Gilfanov, and E. Churazov, High frequencies in the power spectrum of Cyg X-1 in the hard and soft spectral states, *A&A*, in press, 2000.
- Ross R.R., and A.C. Fabian, The effects of photoionization on X-ray reflection spectra in active galactic nuclei, *MNRAS*, **261**, 74-82, 1993
- Ross R.R., A.C. Fabian, and W.N Brandt, X-ray reflection in Galactic black hole candidates: smeared edge profiles and resonant Auger destruction, *MNRAS*, **278**, 1082-1086, 1996.
- Ross R.R., A.C. Fabian, and A.J. Young, X-ray reflection spectra from ionized slabs, *MNRAS*, **306**, 461-466, 1999.
- Różańska A., and B. Czerny, The Structure of the Boundary Layer Between an Accretion Disk and a Corona *AcA*, **46**, 233-252, 1996.
- Różańska A., and B. Czerny, Vertical structure of the accreting two-temperature corona and the transition to an ADAF, *A&A*, **360**, 1170-1186, 2000
- Shakura, N.I., and R.A. Sunyaev, Black holes in binary systems. Observational appearance, *A&A*, **24**, 337-355, 1973.
- Stella L. and M. Vietri, Lense-Thirring Precession and Quasi-periodic Oscillations in Low-Mass X-Ray Binaries, *ApJL*, **492**, L59-L62, 1998.
- Stern B.E., et al., On the Geometry of the X-Ray Emitting Region in Seyfert Galaxies, *ApJL*, **449**, L13-L17, 1995.
- Svensson R., and A.A. Zdziarski, Black hole accretion disks with coronae, *ApJ*, **436**, 599-606, 1994.
- Tanaka Y., and W.H.G. Lewin, Black hole binaries, In X-Ray Binaries, ed. W.H.G. Lewin, J. van Paradijs and E. van den Heuvel, CUP, Cambridge, 126-174, 1995.
- van der Klis M., Rapid aperiodic variability in X-ray binaries, In X-Ray Binaries, eds. W.H.G. Lewin, J. van Paradijs & E. van den Heuvel, CUP, Cambridge, 225-307, 1995
- van der Klis M., Millisecond oscillations in X-ray binaries, *ARA&A*, **38**, 717-760, 2000
- Wilson C.D., and C. Done, Mapping the inner accretion disk of the galactic black hole J1550-564 through its rise to outburst, *MNRAS*, submitted, 2000.
- Zdziarski A.A., P. Lubiński, D.A. Smith, Correlation between Compton reflection and X-ray slope in Seyferts and X-ray binaries, *MNRAS*, **303**, L11-L15, 1999.
- Zdziarski A.A., Radiative Processes and Geometry of Spectral States of Black-Hole Binaries, *IAU Symp.*, **195**, 153-170, Eds., P.C.H. Martens et al., eds, ASP, San Francisco: ASP, 2000
- Zdziarski A.A., et al., , *ApJL*, **438**, 63, 1995.
- Życki P.T., C. Done, and D.A. Smith, Relativistically Smeared X-ray Reprocessed Components in the GINGA spectra of GS2023+338, *ApJL*, **488**, L113-L116, 1997.
- Życki P.T., C. Done, and D.A. Smith, Evolution of the Accretion Flow in Nova Muscae 1991, *ApJL*, **496**, L25-L28, 1998.
- Życki P.T., C. Done, and D.A. Smith, X-ray Spectral Evolution of GS 2023+338 (V404 Cyg) during Decline after Outburst, *MNRAS*, **305**, 231-240, 1999.
- Życki P.T., C. Done, and D.A. Smith, The 1989 May Outburst of the Soft X-ray Transient GS2023+338 (V404 Cyg), *MNRAS*, **309**, 561-575, 1999.
- Życki P.T., and B. Czerny, The Iron K-Alpha Line from a Partially Ionized Reflecting Medium in an Active Galactic Nucleus, *MNRAS*, **266**, 653-668, 1994.